Applied Thermal Engineering 31 (2011) 2885–2893

Contents lists available at ScienceDirect

Applied Thermal Engineering

journal homepage: www.elsevier.com/locate/apthermeng

Thermo-economic optimization of waste heat recovery Organic Rankine Cycles

Sylvain Quoilin [a,*], Sébastien Declaye [a], Bertrand F. Tchanche [b], Vincent Lemort [a]

[a] Thermodynamics Laboratory University of Liège, Campus du Sart Tilman, B49, B-4000 Liège, Belgium
[b] Agricultural University of Athens, 75 Iera Odos Street, 11855 Athens, Greece

ARTICLE INFO

Article history:
Received 18 January 2011
Accepted 9 May 2011
Available online 17 May 2011

Keywords:
Waste Heat Reovery
WHR
Organic Rankine Cycle
ORC
Thermoeconomics
Optimization

ABSTRACT

The present paper focuses both on the thermodynamic and on the economic optimization of a small scale ORC in waste heat recovery application. A sizing model of the ORC is proposed, capable of predicting the cycle performance with different working fluids and different components sizes. The working fluids considered are R245fa, R123, n-butane, n-pentane and R1234yf and Solkatherm. Results indicate that, for the same fluid, the objective functions (economics profitability, thermodynamic efficiency) lead to different optimal working conditions in terms of evaporating temperature: the operating point for maximum power doesn't correspond to that of the minimum specific investment cost: The economical optimum is obtained for n-butane with a specific cost of 2136 €/kW, a net output power of 4.2 kW, and an overall efficiency of 4.47%, while the thermodynamic optimum is obtained for the same fluid with an overall efficiency of 5.22%. It is also noted that the two optimizations can even lead to the selection of a different working fluid. This is mainly due to additional fluid properties that are not taken into account in the thermodynamic optimization, such as the fluid density: a lower density leads to the selection of bigger components which increases the cost and decreases the economical profitability.

1. Introduction

Interest in low-grade heat recovery has grown dramatically in the past decades. An important number of new solutions have been proposed to generate electricity from low temperature heat sources and are now applied to such diversified fields as solar thermal power, industrial waste heat, engine exhaust gases, and domestic boilers. The potential for exploiting waste heat sources from engine exhaust gases or industrial processes is particularly promising [1]: statistical investigations indicate that low-grade waste heat accounts for 50% or more of the total heat generated in industry [2].

Among the proposed solutions, the Organic Rankine Cycle (ORC) system is the most widely used. Its two main advantages are the simplicity and the availability of its components. In such a system, the working fluid is an organic substance, better adapted than water to lower heat source temperatures. Unlike the traditional Rankine power cycles, local and small scale power generation is made possible by ORC technology.

WHR ORCs have been studied in a number of previous works: they generally focused the working fluid selection, which depends strongly on the considered application, and showed that the cycle efficiency is very sensitive to the evaporating pressure [3–5]. Some authors focused on the cycle design, such as Larjola [6] who studied the use of an integrated high speed, oil-free turbogenerator-feed pump for a 100 kWe WHR ORC. Advanced cycle configurations have also been studied: Gnutek et al. [7] proposed an ORC cycle with multiple pressure levels and sliding vane expansion machines using R123 in order to maximize the use of the heat source; Chen et al. [8] studied the transcritical CO2 power cycle as an alternative to the ORC cycle using R123 and showed that the generated output power is slightly higher with the transcritical cycle.

Experimental studies of small scale ORC units demonstrated that volumetric expanders are good candidates for small scale power generation, because of their reduced number of moving parts, reliability, wide output power range, broad availability, and good isentropic effectiveness [9]. In particular, experimental studies on scroll expanders showed very promising results, with reported isentropic effectiveness's ranging from 48 to 68% [10–14]. The screw expander is another very promising solution. It is better adapted to larger capacities and shows the advantage of accepting a high liquid fraction at the inlet, allowing the design of "wet" cycles [15].

Table 1 summarizes the scientific literature in the field of working fluid selection for ORCs: in order to compare the different papers, three characteristics are taken into account: the target application, the considered condensing temperature and the considered evaporating temperature range. The papers comparing

* Corresponding author. Tel.: +32 4 366 48 22; fax: +32 4 366 48 12.
E-mail address: squoilin@ulg.ac.be (S. Quoilin).

1359-4311/$ – see front matter © 2011 Elsevier Ltd. All rights reserved.
doi:10.1016/j.applthermaleng.2011.05.014

Nomenclature

A	area, m^2
c	specific heat, J/(kg K)
d	diameter, mm
h	heat transfer coefficient, W/(m^2 K)
h	specific enthalpy, J/(kg K)
L	length, m
M	mass, kg
$\dot{M}$	mass flow rate, kg/s
N_p	number of plates, -
N_{rot}	rotating speed, rpm
p	pressure, Pa
pinch	pinch point value, K
$\dot{Q}$	Heat power,W
r	ratio,
$r_{v,in}$	Internal built-in volume ratio, -
T	temperature, °C
U	heat transfer coefficient,W/(m^2 K)
v	specific volume, m^3/kg
V	volume, m^3;
V	velocity, m/s
$\dot{V}$	volume flow rate, m^3/s
W	width, m

Greek symbols

ϵ	effectiveness
η	efficiency
ρ	density, kg/m^3

Subscripts and superscripts

amb	Ambient
c	Critical
corr	Correlated
cd	Condenser
em	Eletromechanical
ev	Evaporator
ex	Exhaust
exp	Expander
in	Internal
hr	Heat recovery
htf	Heat transfer fluid
hx	Heat exchanger
l	Liquid
mech	Mechanical
pp	Pump
r	Refrigerant
s	Swept
su	Supply
sf	Secondary fluid
tp	Two-phase
tot	Total
v	Vapor

Acronyms

CHP	Combined Heat and Power
GWP	Global Warming Potential
ICE	Internal Combustion Engine
ODP	Ozone depleting potential
ORC	Organic Rankine Cycle
SIC	Specific Investment Cost
WHR	Waste heat recovery

the working fluid performance as a function of the turbine inlet pressure (see for example [16]) and not the temperature are excluded since the main limitation in the ORC technology is the heat source temperature and not the high pressure.

Table 1 shows that, despite the multiplicity of the working fluid studies, no single fluid has been identified as optimal for the ORC. This is due to the different hypotheses required to perform the fluid comparison:

- Some authors consider the environmental impact (ODP, GWP), the flammability, the toxicity of the working fluid, while some others don't.
- Different working conditions (e.g. the considered temperature ranges) have been assumed, leading to different optimal working fluids.
- The objective functions of the optimization might vary depending on the target application: in CHP or solar applications the cycle efficiency is usually maximized, while in WHR applications, the output power should be maximized [31].

It follows that, since no working fluid can be flagged as optimal, the study of the working fluid candidates should be integrated into the design process of any ORC system.

In many studies [3,4,16,17,20,22,25,27,28,30], it appears that the recommended fluid is the one with the highest critical temperature, i.e. the plant efficiency could be further improved by selecting even higher critical point working fluids [18]. However, a high critical temperature also involves working at specific vapor densities much lower than the critical density. This reduced density shows a high impact on the practical design of the cycle: the components need to be oversized in order to reduce the pressure drops in the heat exchangers and in order for the expansion device to absorb the required volume flow rate. This leads to the conclusion that additional criteria must be added to the sole thermodynamic efficiency when comparing working fluids. This paper aims at addressing this statement by proposing a fluid selection based on thermoeconomic considerations, rather than on a simple thermodynamic objective function.

2. Considered WHR ORC

The simple ORC system integrates four basic components: an evaporator, a turbine/alternator unit, a condenser and a working fluid pump. Although many studies conclude that the introduction of regenerating processes (recuperator, feedliquid heater) increases the cycle efficiency [25,32,33], it has been shown in previous works that this is not justified in waste heat to power applications, for which the power output should be maximized instead of the cycle efficiency [5,31]. The basic configuration is therefore selected in the present work.

The waste heat can be recovered by means of two different setups: (1) direct heat exchange between the waste heat source and the working fluid and (2) a heat transfer fluid loop is integrated to transfer the heat from the waste heat site to the evaporator. In the present study, the heat source is considered to be a generic heat source recovered by a heat transfer fluid loop. The considered system is shown in Fig. 1.

The system boundary is the HTF loop (including its circulating pump) and the heat sink, considered to be cold water. In some cases, dry cooling can be applied at the condenser to save the water

Table 1
Summary of different working fluids studies.

Author(s)	Application	Cond. Temp.	Evap. Temp.	Considered fluids	Recommended fluids
Badr, 1985 [3]	WHR	30–50 °C	120	R11, R113, R114	R113
Maizza and Maizza, 2001 [17]	n/a	35–60 °C	80–110	Unconventional working fluids	R123, R124
Liu et al., 2004 [18]	Waste heat recovery	30 °C	150–200 °C	R123, isopentane, HFE7100, Benzene Toluene, p-xylene	Benzene, Toluene, R123
El Chammas and Clodic, 2005 [19]	ICE	55 °C (100 °C for water)	60–150 °C (150–260 °C for water)	Water, R123, isopentane, R245ca, R245fa, butane, isobutene and R-152a	Water, R245-ca and isopentane
Drescher and Bruggemann, 2007 [20]	Biomass CHP	90 °C[a]	250 - 350 °C[a]	ButylBenzene, Propylbenzene, Ethylbenzene, Toluene, OMTS	ButylBenzene
Hettiarachchia et al., 2007 [21]	Geothermal	30 °C[a]	70–90 °C	Ammonia, n-Pentane, R123, PF5050	Ammonia
Lemort et al., 2007 [22]	Waste heat recovery	35 °C	60–100 °C	R245fa, R123, R134a, n-pentane	R123, n-pentane
Saleh et al., 2007 [23]	Geothermal	30 °C	100 °C	alkanes, fluorinated alkanes, ethers and fluorinated ethers	RE134, RE245, R600, R245fa, R245ca, R601
Borsukiewicz-Gozdur and Nowak, 2007 [24]	Geothermal	25 °C	80–115 °C	propylene, R227ea, RC318, R236fa, ibutane, R245fa	Propylene, R227ea, R245fa
Mago, 2008 [25]	WHR	25 °C	100–210 °C	R113, 123, R245ca, Isobutane	R113
Tchanche et al., 2009 [26]	Solar	35 °C	60–100 °C	Refrigerants	R152a, R600, R290
Facão, 2009 [27]	Solar	45 °C	120 °C/230 °C	Water, n-pentane HFE7100, Cyclohexane, Toluene, R245fa, n-dodecane, Isobutane	n-dodecane
Dai, 2009 [5]	WHR	25 °C	145 °C[a]	Water, ammonia, butane, isobutane R11, R123, R141B, R236EA, R245CA, R113	R236EA
Desai, 2009 [28]	WHR	40 °C	120 °C	Alcanes, Benzene, R113, R123, R141b, R236ea, R245ca, R245fa, R365mfc, Toluene	Toluene, Benzene
Gu, 2009 [4]	WHR	50 °C	80–220 °C	R600a, R245fa, R123, R113	R113, R123
Mikielewicz, 2010 [29] [b]	CHP	50 °C	170 °C	R365mfc, Heptane, Pentane, R12, R141b, Ethanol	Ethanol
Aljundi, 2011 [30]	n/a	30 °C	50–140 °C	RC-318, R-227ea, R-113, isobutane, n-butane, n-hexane, isopentane, neo-pentane, R-245fa, R-236ea, C5F12, R-236fa	n-hexane

[a] Max/min temperature of the heat source/sink instead of evaporating or condensing temperature.
[b] The part of the study evaluating supercritical working fluids has not been taken into account since the present paper focuses on subcritical ORC conditions.

resources, but this case is not considered in the present analysis. Since the methodology proposed in this work aims at being as generic as possible, the HTF heat exchanger is not considered because this component is very heat source dependent: in some cases, the heat exchanger can already be present on the process, and its size and configuration can vary a lot depending on the nature of the heat source.

3. Working fluid candidates

In order to compare a reasonable amount of working fluids a pre-screening of the working fluid candidates is necessary.

From numerous studies related to the selection of fluids for ORC-WHR (see Table 1), a certain number of working fluids characteristics can be outlined. Fluids with high critical temperature or high boiling point such as toluene and silicone oils are usually used with high temperature heat sources (typically close to 300 °C). Hydrocarbons such as pentanes or butanes and refrigerants such as R227ea, R123, R245fa, and HFE7000 are good candidates for moderate and low temperatures (typically lower than 200 °C). Fluids with a high vapor density are advisable as they allow reducing the turbine size and the heat exchangers areas. Additional working fluid characteristics to be taken into account are the flammability, the toxicity, the environmental impact, the cost and the chemical stability (the cycle should always be operated much below the maximum thermal stability temperature).

Presently, only a few working fluids are available on the market and some are being progressively phased out by the Montreal protocol because of their effects on the environment (high Ozone Depleting Potential), reducing the range of choice.

The pre-selection is performed according to the following criteria:

- The working fluid should have a critical temperature lower than 200 °C.
- The aforementioned selection criteria should be fulfilled in an acceptable way. For instance, fluids with a very high ODP (close to 1) are rejected.
- It should be a well-known working fluid in the ORC field, i.e. a fluid that has been previously studied in the scientific

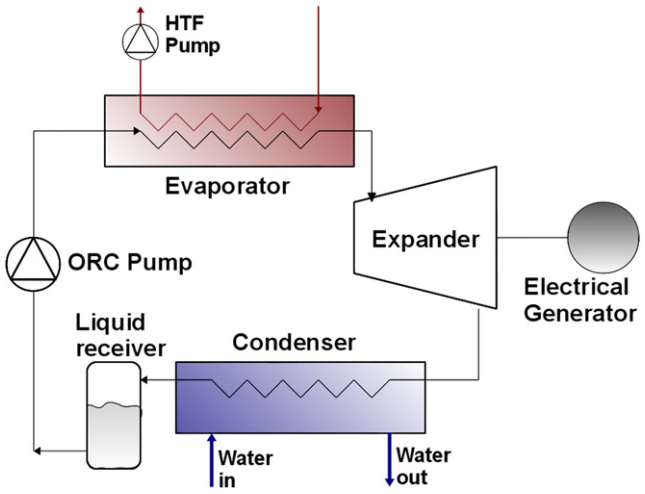

Fig. 1. Considered waste heat recovery ORC system.

literature (cfr. Table 1) or fluids that are used in commercial ORC power plants, such as solkatherm, n-pentane or R134a (see [31] for a review).

It should be noted that R134a is currently being replaced by R1234yf because of its high Global Warming Potential (GWP). HFE7000 and Solkatherm are announced as replacements for R123 due to its non-null Ozone Depleting Potential (ODP): the latter is already or will be phased out at the latest in 2030 depending on national legislations. For the present work, it is decided to include the replacement fluids in the analysis as well as the traditional ones in order to compare their respective performance.

The final selection of working fluid candidates is described in Table 2.

4. Waste heat recovery ORC model

This section describes the modeling of each component of the waste heat recovery ORC. All the models are implemented under the EES environment [34].

4.1. Heat exchangers model

The plate heat exchangers are modeled by means of the Logarithmic Mean Temperature Difference (LMTD) method for counter-flow heat exchangers. They are subdivided into 3 moving-boundaries zones, each of them being characterized by a heat transfer area A and a heat transfer coefficient U, as described in [35].

Table 2
List of considered working fluids.

	ASHRAE 34[a]	GWP	ODP	Tc (°C)	Pc (bar)
R1234yf	A2	4	0	94.75	33.7
R134a	A1	1300	0	101.1	40.6
R-600	A3	20	0	152	37.96
R245fa	B1	950	0	154.1	36.4
HFE7000	n/a	370	0	165	24.8
SES36	n/a	n/a	0	177.6	28.5
R-123	B1	77	0.02	183.7	36.68
R-601	A3	20	0	196.5	33.64

[a] ASHRAE Standard 34 – Refrigerant safety group classification. 1: No flame propagation; 2: Lower flammability; 3: Higher Flammability; A: Lower Toxicity; B: Higher Toxicity.

The heat transfer coefficient U is calculated by considering two convective heat transfer resistances in series (secondary fluid and refrigerant sides).

$$\frac{1}{U} = \frac{1}{h_r} + \frac{1}{h_{sf}} \tag{1}$$

The total heat transfer area of the heat exchanger is given by:

$$A_{tot} = A_l + A_{tp} + A_v = (N_p - 2) \cdot L \cdot W \tag{2}$$

N_p being the number of plates, L the plate length and W the plate width.

4.1.1. Single-phase

Forced convection heat transfer coefficients are evaluated by means of the non-dimensional relationship:

$$\mathrm{Nu} = \mathrm{C}\mathrm{Re}^m\mathrm{Pr}^n \tag{3}$$

where the influence of temperature-dependent viscosity is neglected.

The parameters C, m and n are set according to Thonon's correlation for corrugated plate heat exchangers [36].

The pressure drops are computed with the following relation:

$$\Delta p = \frac{2 \cdot f \cdot G^2}{\rho \cdot D_h} \cdot L \tag{4}$$

Where f is the friction factor, calculated with the Thonon correlation [36], G is the mass velocity (kg/s m^2),ρ is the mean fluid density,D_h is the hydraulic diameter and L is the plate length.

4.1.2. Boiling heat transfer coefficient

The overall boiling heat transfer coefficient is estimated by the Hsieh correlation [37], established for the boiling of refrigerant R410a in a vertical plate heat exchanger. This heat exchange coefficient is considered as constant during the whole evaporation process and is calculated by:

$$h_{tp} = \mathrm{C} \cdot h_l \cdot \mathrm{Bo}^{0.5} \tag{5}$$

Where Bo is the boiling number and h_l is the all-liquid non-boiling heat transfer coefficient.

The pressure drops are calculated in the same manner as in eq. (4), using the Hsieh correlation for the calculation of the friction factor [37].

4.1.3. Condensation heat transfer coefficient

The condensation heat transfer coefficient is estimated by the Kuo correlation [38], established in the case of a vertical plate heat exchanger fed with R410A. It is given by:

$$h_{tp} = C \cdot h_l \cdot \left(0.25 \cdot \mathrm{Co}^{-0.45} \cdot \mathrm{Fr}_l^{0.25} + 75 \cdot \mathrm{Bo}^{0.75}\right) \tag{6}$$

Where Fr_l is the Froude Number in saturated liquid state, Bo the boiling number and Co the convection number.

The pressure drops are calculated in the same manner as in Eq. (4), using the Kuo correlation for the calculation of the friction factor [38].

4.1.4. Heat exchanger sizing

For a given corrugation pattern (amplitude, chevron angle, and enlargement factor), two degrees of freedom are available when sizing a plate heat exchanger: the length and the total flow width. The total flow width is given by the plate width multiplied by the number of channels:

$$W_{tot} = W_{hx} \cdot \frac{N_p - 1}{2} \quad (7)$$

The two degrees of freedom are fixed by the heat exchange area requirement and the limitation on the pressure drop on the working fluid side:

- Increasing the total width decreases the Reynolds number. This leads to a lower pressure drop and to a higher required heat transfer area, since the heat transfer coefficient is also decreased.
- Increasing the plate length leads to a higher pressure drop.

Therefore, by imposing a pinch point and a pressure drop, it is possible to define the total width and the length of the plate heat exchanger. The flow chart of the sizing process is shown in Fig. 2.

The imposed parameters of the model are presented in Table 3.

4.2. Expander model

Volumetric expanders, such as the scroll, screw or reciprocating technologies present an internal built-in volume ratio ($r_{v,in}$) corresponding to the ratio between the inlet pocket volume and the outlet pocket volume.

Under-expansion occurs when the internal pressure ratio imposed by the expander is lower than the system pressure ratio. In that case, the pressure in the expansion chambers at the end of the expansion process (P_{in}) is higher than the pressure in the discharge line.

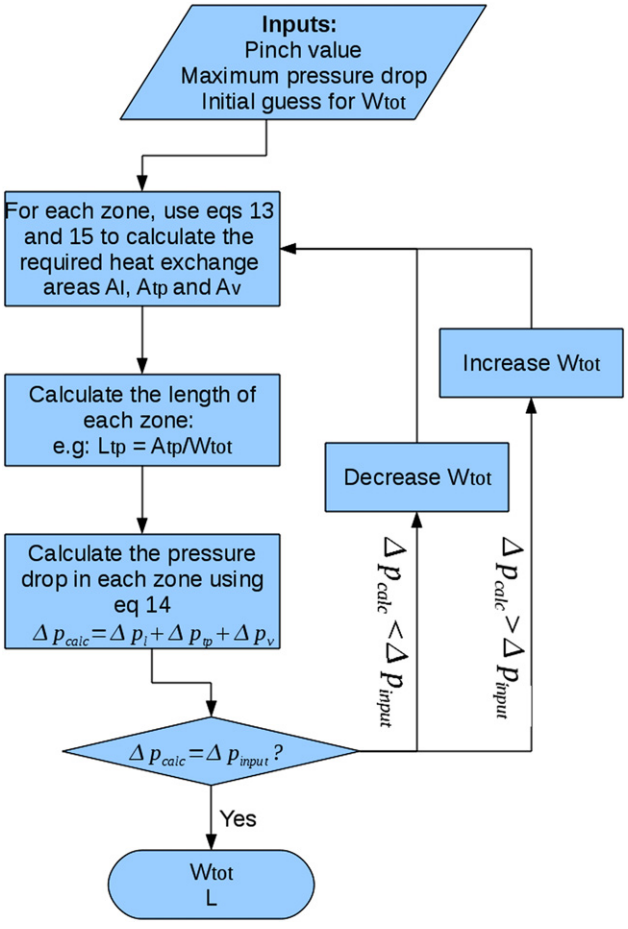

Fig. 2. Flow chart of the heat exchanger sizing process.

Table 3
Heat exchanger model parameters.

Parameter	Description	Value
D_h	Hydraulic diameter	2 mm
$\beta_{chevron}$	Chevron angle	45°

Over-expansion occurs when the internal pressure ratio imposed by the expander is higher than the system pressure ratio.

Under and over-expansion losses can be modeled by splitting the expansion into two consecutive steps [12]:

- Isentropic expansion:

$$w_1 = h_{su} - h_{in} \quad (8)$$

h_{in} being the isentropic enthalpy at pressure p_{in}.

- Constant volume expansion:

$$w_2 = v_{in} \cdot (p_{in} - p_{ex}) \quad (9)$$

w_2 is positive in case of under-expansion, and negative in case of over-expansion.

The total expansion work is then obtained by summing w_1 and w_2.

Other losses such as internal leakage, supply pressure drop, heat transfers and friction are lumped into one single mechanical efficiency η_{mech}:

$$\dot{W}_{exp} = \dot{M} \cdot (w_1 + w_2) \cdot \eta_{mech} \quad (10)$$

And, since the expansion is assumed adiabatic:

$$h_{ex} = h_{su} - \frac{\dot{W}_{exp}}{\dot{M}} \quad (11)$$

For given rotational speed and fluid flow rate, the expander swept volume is recalculated by the model with the following equation:

$$\dot{M} = \frac{\rho_{su} \cdot V_s \cdot N_{rot}}{60} \quad (12)$$

4.3. Pumps model

Two pump consumptions are taken into account: the heat transfer fluid pump and the working fluid pump. They are modeled by their isentropic efficiency, defined by:

$$\epsilon_{pp} = \frac{\Delta h_{s,pp}}{\Delta h_{pp}} = \frac{v_{su,pp} \cdot \left(p_{ex,pp} - p_{su,pp}\right)}{h_{ex,pp} - h_{su,pp}} \quad (13)$$

For the HTF pump, the pressure difference is given by the pressure drop in the evaporator while for the ORC pump, it is given by the difference between evaporating and condensing pressures. A constant, realistic value of 60% is assumed for the pump efficiency [39].

4.4. Cycle model

The global model of the system is obtained by interconnecting each subcomponent model. Several performance indicators can be defined.

The overall heat recovery efficiency:

$$\epsilon_{hr} = \frac{\dot{Q}_{ev}}{\dot{Q}_{ev,max}} = \frac{\dot{M}_{HTF} \cdot \bar{c}_{p,htf} \cdot \left(T_{htf,su,ev} - T_{htf,ex,ev}\right)}{\dot{M}_{HTF} \cdot \bar{c}_{p,htf} \cdot \left(T_{htf,su,ev} - T_{amb}\right)} \quad (14)$$

The net electrical output power:

$$\dot{W}_{net} = \dot{W}_{exp} - \dot{W}_{pp} - \dot{W}_{pp,htf} \quad (15)$$

The ORC cycle efficiency:

$$\eta_{ORC} = \frac{\dot{W}_{net}}{\dot{Q}_{ev}} \quad (16)$$

The overall system efficiency:

$$\eta_{overall} = \frac{\dot{W}_{net}}{\dot{M}_{HTF} \cdot \bar{c}_{p,htf} \cdot \left(T_{htf,su,ev} - T_{amb}\right)} = \epsilon_{hr} \cdot \eta_{ORC} \quad (17)$$

For the present study, the following assumptions are made:

- The heat source is exhaust gas at 180 °C, with a mass flow rate of 0.3 kg/s. The heat transfer fluid is TherminolVP-1.
- The condenser is cooled with cold water at 15 °C, and a flow rate of 0.5 kg/s.
- The superheating at the expander inlet is 5 K.
- The subcooling after the condenser is 5 K.
- The internal built-in volume ratio of the scroll expander is 3.4.
- The expander mechanical efficiency, 70%.
- The isentropic efficiency of the pump, 60%.

5. Thermodynamic optimization

In the present case of an ORC designed for a waste heat recovery application, the thermodynamic optimization aims at maximizing the net power output. This is equivalent to maximizing the overall efficiency since the flow rate and the temperature of the heat source are fixed in Eq. (17). For the purpose of this optimization, the pinch points on the heat exchangers must be imposed. A value of 10 K is selected for both the condenser and the evaporator. The pressure drop is set to 100 mbar on the evaporator and on 200 mbar on the condenser.

As a general rule, the following statements should be taken into account:

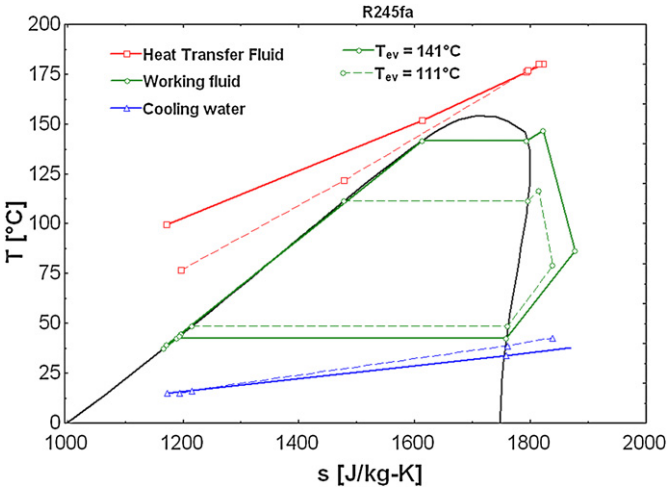

Fig. 3. T-s diagram of the cycle for two different Tev.

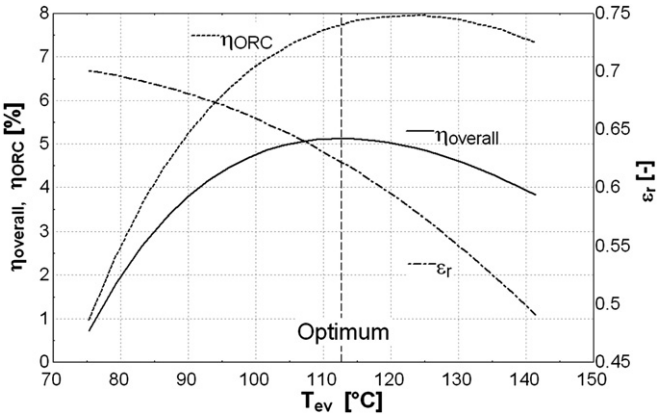

Fig. 4. Influence of T_{ev} on the performance indicators.

- The condensing temperature should be maintained as low as possible.
- The superheating at the evaporator exhaust should be as low as possible when using high molecular weight organic fluids [5,25,40].
- The optimal evaporation temperature results of an optimization of the overall heat recovery efficiency (see below) [5,18,41].

In this case, the only available degree of freedom is the evaporating temperature. Increasing the evaporation temperature implies several antagonist effects:

- The under-expansion losses in the expander are increased, and its efficiency is decreased.
- The heat recovery efficiency is decreased since the heat source is cooled down to a higher temperature. This is shown in Fig. 3: the dashed cycle operates at a lower evaporating temperature, and more heat is recovered from the heat source.
- The expander specific work is increased since the pressure ratio is increased.

These influences are illustrated for the case of R245fa in Fig. 4. For this particular steady-state working point, an optimum evaporation temperature of 113 °C is obtained.

This analysis can be conducted for each candidate working fluid in order to define the optimum evaporation temperature. The results of this optimization are presented in Table 4. n-butane is the fluid showing the highest overall efficiency, followed by R245fa and R123. It should be noted that, in the case of R134a and R1234yf, the optimization lead to increase the evaporating temperature up to the critical point. It is therefore obvious that these two fluids are not suitable for the present heat source temperature.

Table 4
Performance of the different working fluids.

Fluid	T_{ev} [°C]	$\eta_{overall}$ [%]	η_{ORC} [%]	W_{net} [W]
R123	111.8	5.004	8.412	4648
n-butane	114.4	5.222	7.977	4851
SES36	110.4	4.803	7.357	4462
HFE-7000	111.6	4.928	6.857	4577
R245fa	113.5	5.128	7.779	4764
n-pentane	111.6	4.933	8.071	4583
R134a	100.9	3.919	5.193	3640
R1234yf	91.34	2.734	3.616	2540

6. Thermoeconomic optimization

The goal of this section is to propose an alternative optimization for the ORC working conditions: instead of the system efficiency, the selected objective function for this optimization is the specific investment cost (SIC) expressed in €/KWe:

$$\mathrm{SIC} = \frac{\mathrm{Cost}_{\mathrm{Labor}} + \mathrm{Cost}_{\mathrm{Components}}}{\dot{W}_{\mathrm{net}}} \quad (18)$$

Since WHR sources are cost-free by definition, optimizing this parameter is equivalent to optimizing the profitability of the system if maintenance and insurance annual costs are neglected.

In order to obtain the total investment cost, a cost correlation is used for each component of the system and is given in Table 5.

The cost of the expander is based on the cost of hermetic compressors with the same swept volume. It has indeed been showed in previous publications that turning volumetric compressors (such as scroll compressors) into expanders is feasible with a good efficiency [10–14]. In order to take into account the lower maturity of the expander technology, the cost of the compressor is multiplied by a factor 1.5 to obtain the cost of the expander. The costs used to establish the correlations for the compressor and the heat exchangers are based on the Belgian prices in 2010. The pump cost correlation is an exponential expression, proposed by Bejan [42]. It shows the advantage of requiring cost data for only one pump, and assumes that this cost can be correlated to the nominal power as single input. For the present analysis, the capacity of the liquid receiver is assumed to be constant at 5 L. The pipe diameter is calculated by imposing the fluid speed to the values recommended in refrigeration applications: $V_{ex,pp} = V_{ex,cd} = 0.6$ m/s; $V_{ex,ev} = 10$ m/s; $V_{ex,exp} = 12$ m/s. The lengths of the liquid, low pressure vapor and high pressure vapor are assumed to be 3 m, 1 m and 1 m respectively. The total mass of working fluid in the system is calculated by assuming that the two-phase zone in the heat exchangers is half-filled with liquid, and by assuming that one third of the liquid receiver is filled with liquid.

6.1. Influence of the working conditions

Contrary to the thermodynamic optimization, the thermoeconomic optimization allows defining more cycle parameters than the sole evaporating temperature: the pressure drops and the pinch points on the heat exchangers also result from an economic optimum. The influence of these two parameters is straightforward:

- Decreasing the pressure drop requires increasing the total width W_{tot} of the heat exchanger, and therefore its cost. On the other hand, the cycle efficiency is increased which decreases the SIC.
- A lower pinch point requires a higher heat exchange area, which also increases the cost of the system. On the other hand, the evaporating and condensing pressures are respectively increased and decreased, which increases the output power.

The influence of the evaporating temperature on the cost is manyfold. In general, increasing this parameter increases the vapor density which reduces the pressure drops in the heat exchangers and the required swept volume of the expander. This is illustrated in Fig. 5: the cost of the expander decreases with the evaporation temperature, but the cost of the working fluid pump increases since the pressure difference increases. The influence on the cost of the other components is more limited.

Fig. 6 shows the evolution of the SIC with the evaporating temperature. A minimum value for the SIC is observed around 136 °C for the particular case of R245fa. However, this minimum

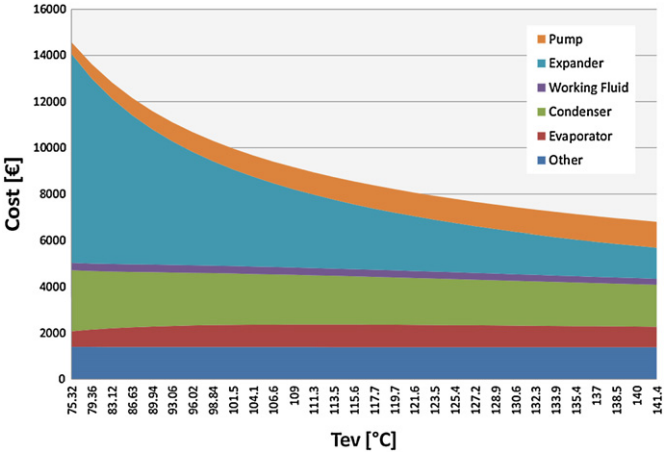

Fig. 5. Influence of T_{ev} on the component costs.

Table 5
Component costs.

Component	Dependent variable	Cost [€]
Expander	Volume flow rate $\dot{V}_{su,exp}$ (m^3/s)	$1.5 \cdot (225 + 170 \cdot \dot{V}_{su,exp})$
Heat exchangers	Heat exchange area A (m^2)	$190 + 310 \cdot A$
Working fluid pump	Electrical power $\dot{W}_{pp}$ (W)	$900 \cdot (\dot{W}_{pp}/300)^{0.25}$
HTF pump	Electrical power $\dot{W}_{pp}$ (W)	$500 \cdot (\dot{W}_{pp}/300)^{0.25}$
Liquid receiver	Volume Vol (l)	$31.5 + 16 \cdot \mathrm{Vol}$
Piping	Pipe diameter d_{pipe} (mm)	$(0.897 + 0.21 \cdot d_{pipe}) \cdot L_{pipe}$
Working fluid	Mass M (kg)	$20 \cdot M$
Miscellaneous hardware	/	300
Control system	/	500
Labor	Total component costs (€)	0.3 TCC

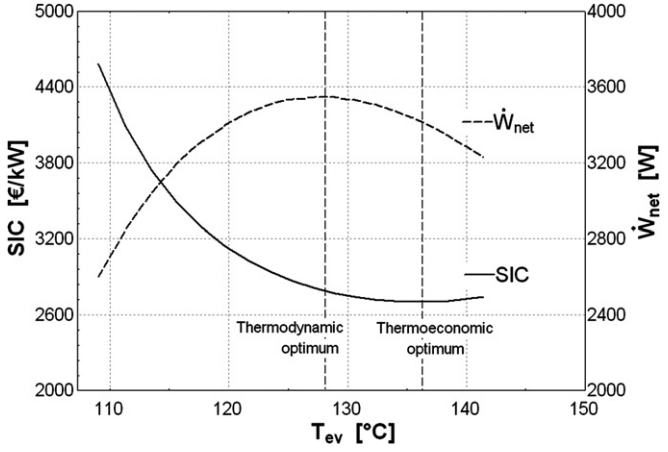

Fig. 6. Thermodynamic and thermoeconomic optimizations for R245fa.

Table 6
Results of the thermoeconomic optimization.

Fluid	T_{ev}	$\eta_{overall}$	η_{ORC}	$pinch_{cd}$	$pinch_{ev}$	ΔP_{cd}	ΔP_{ev}	SIC
	°C	–	–	K	K	mbar	mbar	€/kW
R245fa	135.9	3.687	6.964	28.33	7.834	449	261	2700
n-butane	133.2	4.474	7.686	18.31	7.506	357	69	2136
HFE-7000	142.4	3.349	6.123	31.84	6.164	297	807	3069
n-pentane	139.9	3.878	8.369	21.81	4	172	146	2505
R123	141.4	3.427	8.298	30.28	4.967	268	507	2916
R134a	101.1	3.017	5.796	13.47	51.68	527	12	3432
R1234yf	94.42	2.404	5.12	12.1	62.14	398	8	4260
SES36	141.6	3.461	7.137	31.47	4	154	127	2659

does not coincide with maximum output power of 4325 W obtained at 128 °C. This observation can be extended to other fluids used in this investigation.

The five parameters (P_{ev}, $pinch_{cd}$, $pinch_{ev}$, ΔP_{cd}, ΔP_{ev}) are therefore optimized with the objective of minimizing the SIC. This is done using the simplex algorithm [43]. Table 6 shows the results of the thermoeconomic optimization for each fluid. As for the thermodynamic optimization, R134a and R1234yf were limited by their critical temperature. For the other fluids, the optimization leads to a much higher optimal evaporating temperature than in the first case (about 25 °C higher). The optimal pinch point on the evaporator is always below 10 K, except for R134a and R1234yf, again because of the critical temperature limitation. It is however much higher on the condenser, with values comprised between 20 and 30 K, due to the lower density of the fluid and to higher pressure drops in the low pressure vapor. It is interesting to note that the optimum fluid is (n-butane) is the same as in the thermodynamic optimization.

7. Conclusion

Fluid selection for the Organic Rankine Cycle is an important issue and is very dependent on the target application, on the working conditions and even on the criteria taken into account.

In this work, a thermodynamic model of a waste heat recovery ORC has been developed in order to compare both the thermodynamic and the thermoeconomic performance of several typical working fluids for low to medium temperature-range ORCs.

The thermodynamic optimization leads to the selection of the following working fluids, sorted by overall efficiency (highest efficiency first): n-butane, R245fa, R123, n-pentane, HFE7000, SES36, R134a, R1234yf. The thermoeconomic optimization leads to the selection of the following working fluid, sorted by Specific Investment Cost (lowest first): n-butane, n-pentane, SES36, R245fa, R123, HFE7000, R134a, R1234yf. The economical optimum is obtained with a specific cost of 2136 €/kW and an overall efficiency of 4.47%, while the thermodynamic optimum is obtained with an overall efficiency of 5.22%.

The following statements can be formulated:

- Despite the large amount of working fluid studies for ORC applications, their conclusions do not lead to one single optimal fluid for a given temperature level and a given application.
- When optimizing the thermodynamic performance of a WHR ORC, an optimum evaporating temperature exists that maximizes the output power (or the overall efficiency). The optimal evaporating temperature is usually far below the heat source temperature.
- The thermoeconomic optimization leads to the selection of a higher evaporating temperature, because it increases the high-pressure vapor density and decreases the cost of the expander and of the evaporator.
- For the particular working conditions selected for the work, both optimizations lead to the selection of n-butane as optimal fluid. However, the "second-best fluid" differs for both optimization, as well as the next ones. Therefore, if the thermodynamic optimization can give a good idea of the best fluids, it won't necessarily lead to the selection of the optimal working fluid in terms of economical profitability.

It should be noted that the present study mainly aims at describing a methodology, rather than an accurate economic study for small-scale WHR ORCs: the cost taken into account correspond to the retail price for Belgium, but a large-scale commercialization of such systems could dramatically reduce those costs. On the other hand, some costs were not taken into account, such as the cost of the HTF heating system, because this cost is very dependent on the target application.

References

[1] J.F. Wang, Y.P. Dai, et al., Exergy analyses and parametric optimizations for different cogeneration power plants in cement industry, Applied Energy 86 (6) (2009) 941–948.
[2] T.C. Hung, T.Y. Shai, S.K. Wang, A review of Organic Rankine Cycles (ORCs) for the recovery of low-grade waste heat, Energy 22 (1997) 661–667.
[3] O. Badr, P.W. Ocallaghan, et al., Rankine-Cycle systems for Harnessing power from low-grade energy-Sources, Applied Energy 36 (1990) 263–292.
[4] W. Gu, Y. Weng, Y. Wang, B. Zheng, Theoretical and experimental investigation of an Organic Rankine Cycle for a waste heat recovery system, Part A: Journal of Power and Energy 223 (2009) 523–533 Proc. IMechE.
[5] Y.P. Dai, J.F. Wang, et al., Parametric optimization and comparative study of Organic Rankine Cycle (ORC) for low grade waste heat recovery, Energy Conversion and Management 50 (2009) 576–582.
[6] J. Larjola, Electricity from industrial waste heat using high-speed Organic Rankine Cycle (ORC), International Journal of Production Economics 41 (2009) 227–235.
[7] Z. Gnutek, A. Bryszewska-Mazurek, The thermodynamic analysis of multicycle ORC engine, Energy 26 (2001) 1075–1082.
[8] Y. Chen, P. Lundqvist, et al., A comparative study of the carbon dioxide transcritical power cycle compared with an Organic Rankine Cycle with R123 as working fluid in waste heat recovery, Applied Thermal Engineering 26 (2006) 2142–2147.
[9] R. Zanelli, D. Favrat, Experimental investigation of a hermetic scroll expander-generator, in: Proceedings of the International Compressor Engineering Conference at Purdue, 1994, pp. 459–464.
[10] D. Manolakos, G. Papadakis, S. Kyritsis, K. Bouzianas, Experimental evaluation of an autonomous low-temperature solar Rankine cycle system for reverse osmosis desalination, Desalination 203 (2007) 366–374.
[11] B. Aoun, D. Clodic, Theoretical and experimental study of an oil-free scroll type vapor expander, in: Proceedings of Nineteenth International Compressor Engineering Conference at Purdue, 2008, paper 1188.
[12] V. Lemort, S. Quoilin, C. Cuevas, J. Lebrun, Testing and modeling a scroll expander integrated into an Organic Rankine Cycle, Applied Thermal Engineering 29 (2009) 3094–3102.
[13] T. Yanagisawa, Y.Fukuta, T. Ogi, T. Hikichi, Performance of an oil-free scroll-type air expander, in: Proceedings Of the ImechE Conference Transactions On Compressors and Their Systems, 2001, pp. 167–174.
[14] El.H. Kane, Intégration et optimisation thermoéconomique & environomique de centrales thermiques solaires hybrides, PhD thesis, Laboratoire d'Energétique Industrielle, Ecole polytechnique Fédérale de Lausanne, 2002.
[15] I.K. Smith, N. Stosic, A. Kovacevic, Steam as the working fluid for power recovery from exhaust gases by the use of screw expanders, in: Proceedings of The International Conference on Compressors and their Systems, London, 2009.
[16] T.C. Hung, Waste heat recovery of Organic Rankine Cycle using dry fluids, Energy Conversion and Management 42 (2001) 539–553.
[17] V. Maizza, A. Maizza, Unconventional working fluids in organic Rankine-cycles for waste energy recovery systems, Applied Thermal Engineering 21 (2001) 381–390.
[18] B.-T. Liu, K.-H. Chien, C.-C. Wang, Effect of working fluids on Organic Rankine Cycle for waste heat recovery, Energy 29 (2004) 1207–1217.
[19] R. El Chammas, D. Clodic, Combined Cycle for Hybrid Vehicles. Society of Automotive Engineers (SAE), 2005.
[20] U. Drescher, D. Bruggemann, Fluid selection for the Organic Rankine Cycle (ORC) in biomass power and heat plants, Applied Thermal Engineering 27 (2007) 223–228.

[21] H.D.M. Hettiarachchia, M. Golubovica, W.M. Worek, Optimum design criteria for an Organic Rankine Cycle using low-temperature geothermal heat sources, Energy 32 (9) (2007) 1698–1706.
[22] V. Lemort, C. Cuevas, J. Lebrun, I.V. Teodorese, Contribution à l'étude des cycles de Rankine de récupération de chaleur, VIIIème Colloque Inter-universitaire Franco-Québécois sur la Thermique des Systèmes, Montréal, Canada, 2007.
[23] B. Saleh, G. Koglbauer, M. Wendland, J. Fischer, Working fluids for low-temperature Organic Rankine Cycles, Energy 32 (2007) 1210–1221.
[24] A. Borsukiewicz-Gozdur, W. Nowak, Comparative analysis of natural and synthetic refrigerants in application to low temperature Clausius-Rankine Cycle, Energy 32 (2007) 344–352.
[25] P.J. Mago, L.M. Chamra, K. Srinivasan, C. Somayaji, An examination of regenerative Organic Rankine Cycles using dry fluids, Applied Thermal Engineering 28 (2008) 998–1007.
[26] B.F. Tchanche, G. Papadakis, G. Lambrinos, A. Frangoudakis, Fluid selection for a low-temperature solar Organic Rankine Cycle, Applied Thermal Engineering 29 (2009) 2468–2476.
[27] J. Facão, A. Palmero-Marrero, A.C. Oliveira, Analysis of a solar assisted micro-cogeneration ORC system, International Journal of Low Carbon Technologies 3/4 (2009).
[28] N.B. Desai, S. Bandyopadhyay, Process integration of Organic Rankine Cycle, Energy 34 (2009) 1674–1686.
[29] D. Mikielewicz, J. Mikielewicz, A thermodynamic criterion for selection of working fluid for subcritical and supercritical domestic micro CHP, Applied Thermal Engineering 30 (2010) 2357–2362.
[30] I.H. Aljundi, Effect of dry hydrocarbons and critical point temperature on the efficiencies of Organic Rankine Cycle, Renewable Energy 36 (2011) 1196–1202.
[31] S. Quoilin, V. Lemort, Technological and Economical Survey Of Organic Rankine Cycle systems, in: Fifth European Conference on Economics and Management of Energy in Industry, Vilamoura, Portugal, 2009.
[32] G. Angelino, M. Gaia, E. Macchi, A review of Italian activity in the field of Organic Rankine Cycles, VDI Berichte 539 (1984) 465–482.
[33] A. McMahan, Design & Optimization of Organic Rankine Cycle Solar-Thermal Powerplants, Master of Science thesis, Madison, WI, 2006.
[34] S.A. Klein, Engineering Equation Solver. F-Chart Software, Middleton, WI, 2010.
[35] S. Quoilin, V. Lemort, J. Lebrun, Experimental study and modeling of an Organic Rankine Cycle using scroll expander, Applied Energy 87 (2010) 1260–1268.
[36] B. Thonon, R. Vidil, C. Marvillet, Recent Research and Developments in plate heat-Exchangers, Journal of Enhanced Heat Transfer 2 (1995) 149–155.
[37] Y.Y. Hsieh, T.F. Lin, Saturated flow boiling heat transfer and pressure drop of refrigerant R-410A in a vertical plate heat exchanger, International Journal of Heat and Mass Transfer 45 (2002) 1033–1044.
[38] W.S. Kuo, Y.M. Lie, Y.Y. Hsieh, T.F. Lin, Condensation heat transfer and pressure drop of refrigerant R410a flow in a vertical plate heat exchanger, International Journal of Heat and Mass Transfer 48 (2005) 5205–5220.
[39] Lin, C., Feasibility of using power steering pumps in small-scale solar thermal electric power systems, S.B. thesis Dept. Of Mechanical Engineering, MIT, 2008.
[40] T. Yamamoto, T. Furuhata, N. Arai, K. Mori, Design and testing of the Organic Rankine Cycle, Energy 26 (2001) 239–251.
[41] A.A. Lakew, O. Bolland, Working fluids for low-temperature heat source, Applied Thermal Engineering 30 (2010) 1262–1268.
[42] A. Bejan, G. Tsatsaronis, M. Moran, Thermal Design and Optimization. John Wiley & Sons, 1996.
[43] J. Kiefer, Sequential minimax search for a maximum, Proceedings of the American Mathematical Society 4 (1953) 502–506.